Séminaire Lotharingien de Combinatoire **XX** (2026)
Article #81, 12 pp.

Proceedings of the 38th Conference on Formal Power Series and Algebraic Combinatorics (Seattle)

Web bases, pocket complexes, and affine buildings

Christian Gaetz*[1], Jessica Striker†[2], Joshua P. Swanson‡[3], and Haihan Wu§[4]

[1]*Department of Mathematics, University of California, Berkeley, CA*
[2]*Department of Mathematics, North Dakota State University, Fargo, ND*
[3]*Department of Mathematics, University of Southern California, Los Angeles, CA*
[4]*Department of Mathematics, Johns Hopkins University, Baltimore, MD*

Abstract. A major research program in combinatorial representation theory is to produce effectively computable graphical calculi which fully encode representation categories of interest. Recent work of Gaetz–Pechenik–Pfannerer–Striker–Swanson introduced *fully reduced* 4*-row hourglass plabic graphs*, which, together with work of Cautis–Kamnitzer–Morrison, completes this program for $U_q(\mathfrak{sl}_4)$. These objects come with certain *moves*. Here we build on work of Fontaine–Kamnitzer–Kuperberg and describe how each such move-class may be assembled into a certain highly structured 3-dimensional simplicial complex we call a *pocket*. One of the many remarkable properties of pockets is that they embed in the affine building $\Delta(\mathrm{SL}(4)^\vee)$. This is a very complicated, uncountable simplicial complex built from the affine Grassmannian and intimately involved in the geometric Satake correspondence. Pockets provide finite models for the geometry of this building. Furthermore, pockets possess $\mathrm{SL}(4)$-weight-valued geodesics and are $\mathrm{CAT}(0)$ spaces. Special cases include the well-known tetrahedral-octahedral honeycomb. Pockets are a source of distributive lattices, including alternating sign matrices, tilings of the Aztec diamond, plane partitions, and more.

Keywords: web, affine building, pocket, hourglass plabic graph, plane partition, alternating sign matrix

1 Introduction

1.1 Graphical calculi and web bases

The representation theory of classical groups is one of the centerpieces of modern mathematics and is of fundamental interest in particle physics and quantum mechanics. The

*gaetz@berkeley.edu. Gaetz was partially supported by NSF grant DMS-2452032 and by a travel grant from the Simons Foundation.

†jessica.striker@ndsu.edu. Striker was partially supported by Simons Foundation gift MP-TSM-00002802 and NSF grant DMS-2247089.

‡swansonj@usc.edu. Swanson was partially supported by NSF grant DMS-2348843.

§hwu125@jhu.edu. Wu was supported by NSF grant CCF-2317280 and Simons Foundation grant 994328.

mathematical physicist Roger Penrose introduced a graphical calculus for tensors [14], with roots in earlier work (see, e.g., [13]). A modern incarnation of this idea such as [3, §2] uses certain diagrams to encode morphisms between $\mathrm{SL}(r)$-modules. For instance, the natural $\mathrm{SL}(r)$-equivariant pairing $V \otimes V^* \to \mathbb{C}$ where $V \cong \mathbb{C}^r$ may be represented by a cup "$\cup$" from a black vertex on the left to a white vertex on the right. While we do not require precise details here, the general idea is to find a graphical model where an arbitrary morphism in a category of interest can be written as a sum of diagrams and then manipulated pictorially. Such diagrams are sometimes called *webs*.

One naturally desires such a web calculus to be effectively computable, e.g., to have some reasonably efficient, deterministic algorithm to decide equality of the underlying morphisms. For $\mathrm{SL}(r)$-modules (and indeed the quantum deformation $U_q(\mathfrak{sl}_r)$), Cautis–Kamnitzer–Morrison [3] gave such a calculus by giving a generating set of relations. This situation is akin to having generators for an ideal but no Gröbner basis. For $r = 2$ and $r = 3$, the Temperley–Lieb web basis and Kuperberg's *non-elliptic web basis* [12] may be used to test equality, respectively. A basis with explicit reduction rules for $r = 4$ was recently constructed by Gaetz–Pechenik–Pfannerer–Striker–Swanson [7, Thm. 7.2].

1.2 Fully reduced hourglass plabic graphs

The key new combinatorial objects in [7] build on Postnikov's *plabic graphs* [15]. See Figure 3 (left) for an example.

Definition 1.1 ([7])**.** An *hourglass plabic graph* is a planar graph embedded in a disk with properly colored black or white vertices, where edges may be *hourglasses*, certain half-twist multi-edges. For simplicity we take all boundary vertices to be black and incident to a single non-hourglass edge. An hourglass plabic graph is *r-row* if each internal vertex is r-valent, counting with hourglass multiplicity.

Plabic graphs come with a single *trip permutation* obtained by starting at a boundary vertex and taking a left at white vertices and a right at black vertices. Similarly, r-row hourglass plabic graphs have $(r-1)$ trip permutations trip_i for $i = 1, \ldots, r-1$ obtained by taking the i-th left at white vertices and the i-th right at black vertices; see [7, Fig. 1] and Figure 3 (left) for examples. A 4-row hourglass plabic graph is *fully reduced* if it satisfies certain forbidden crossing conditions [7, Def. 3.30], e.g., no trip_i can cross itself, and no trip_1 can double cross a trip_2. Two r-row hourglass plabic graphs G_1, G_2 are *trip-equivalent* if $\mathrm{trip}_i(G_1) = \mathrm{trip}_i(G_2)$ for all $1 \leq i \leq r-1$.

The main combinatorial result [7, Thm. B] is a bijection between trip-equivalence classes of fully reduced 4-row hourglass plabic graphs and 4-row rectangular standard Young tableaux; see Figure 3 (left) and [7, Fig. 1] examples. Moreover, two trip-equivalent graphs are related by a series of *square moves* or *benzene moves*; see Figure 1 (left). Write $\mathcal{C}(T)$ for the move-class (equivalently, trip-class) associated to a tableau T.

A key feature of the bijection $T \mapsto \mathcal{C}(T)$ is that it intertwines tableau *promotion* with web rotation. The equality testing algorithm in [7, Thm. 7.2] seeks out certain *top* representatives of $\mathcal{C}(T)$.

1.3 Moves, dual diskoids, and pockets

Following a suggestion of Kuperberg, we show that in fact the move-classes $\mathcal{C}(T)$ for $T \in \mathrm{SYT}(4 \times c)$ may be assembled into 3-dimensional simplicial complexes. For this purpose, we first must uncontract each 4-valent vertex into a pair of trivalent vertices connected by a pair of double 2-hourglasses. This may be done in two ways, leading to *IH moves* in addition to square and benzene moves, though this preserves trip-equivalence; see Figure 1 (upper left).

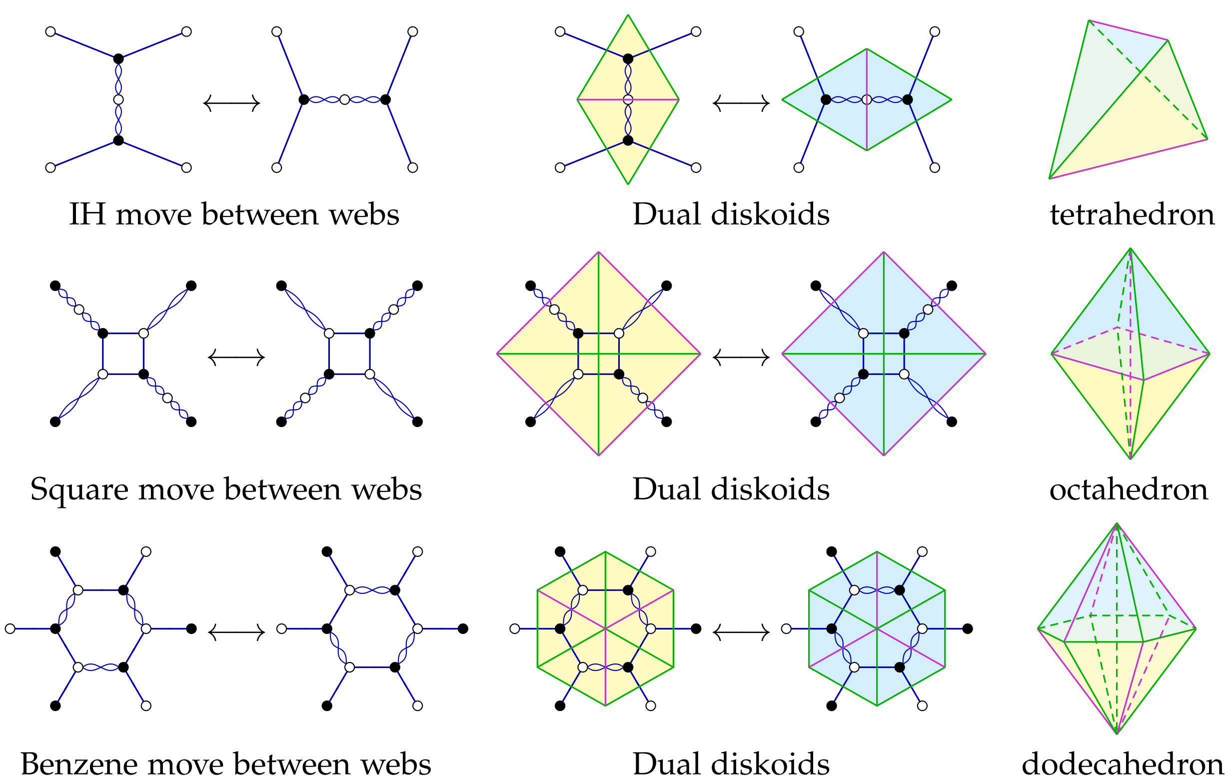

Figure 1: (Left) Moves for 4-row hourglass plabic graphs. (Middle) Corresponding dual diskoids. (Right) Corresponding fragments of pockets. Vertical edges are drawn in the octahedron and dodecahedron.

Definition 1.2 (See [6])**.** The *dual diskoid* of an uncontracted 4-row hourglass plabic graph G is the 2-dimensional simplicial complex $D(G)$ whose vertices are faces of G and edges correspond to adjacent faces. See Figure 1 (middle) for some examples.

Note for later use that every uncontracted vertex has two simple edges and one 2-hourglass. Correspondingly, every triangle in Figure 1 has two green and one red edge.

We now come to our central, new construction. Several examples follow.

Definition 1.3. The *pocket* of a move-class $\mathcal{C}$ of fully reduced 4-row hourglass plabic graphs is the simplicial complex $P(\mathcal{C})$ obtained by gluing together the dual diskoids $D(G)$ for $G \in \mathcal{C}$ by attaching tetrahedra between the portions involved in a move; see Figure 1 (right). For IH moves, this gives a single tetrahedron. For square moves, this gives 4 tetrahedra arranged in an octahedral configuration around a *vertical edge* between the top and bottom of the octahedron. For benzene moves, this gives 6 tetrahedra arranged in a (non-regular) dodecahedron around a vertical edge.

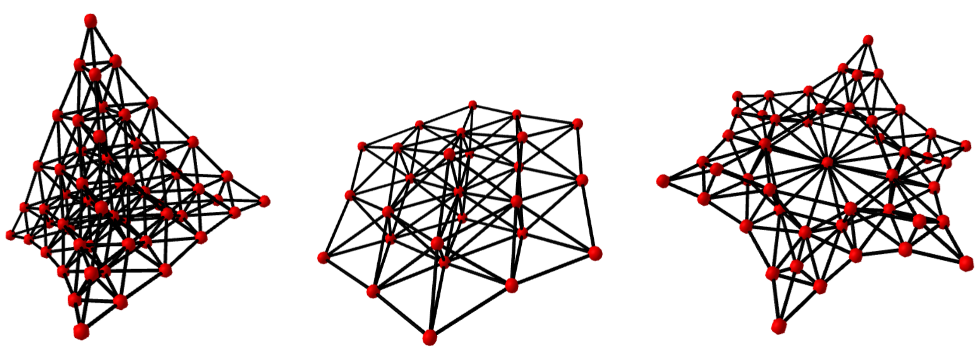

Figure 2: The “alternating sign matrix”, “plane partition”, and “chained hexagon” pockets as bare simplicial complexes.

Example 1.4. In [7, §8], it was shown that the contracted move-class associated to the “superstandard” 4-row rectangular tableau with n columns filled row-by-row is in bijection with the $n \times n$ *alternating sign matrices*. The corresponding pocket for $n = 5$ is drawn in Figure 2 (left), which involves 429 alternating sign matrices, 114432 uncontracted fully reduced webs, and $5^3 = 125$ tetrahedra. Indeed, if one keeps track of which portions come from square moves and which come from IH moves, this is the well-known *tetrahedral-octahedral honeycomb*; see Figure 3 (right) for the $n = 3$ version. This structure has appeared before, e.g., Knutson–Tao–Woodward [11] use “excavation” in this honeycomb along with hives to prove the Littlewood–Richardson rule.

Remark 1.5. In the tetrahedral-octahedral honeycomb, if one disregards all tetrahedra coming from IH moves at white vertices, the order relations among the octahedra and remaining tetrahedra of the pocket form the poset of join irreducibles of the lattice of domino tilings of the Aztec diamond, as in [4, Figure 10]. The octahedra alone correspond to the join irreducibles of the alternating sign matrix poset [4, 17].

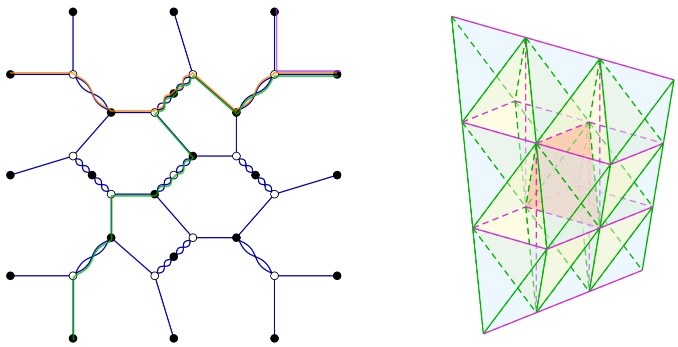

$T =$

1	2	3
4	5	6
7	8	9

Figure 3: (Left) An uncontracted 4-row fully reduced hourglass plabic graph associated to the 3×3 alternating sign matrix with a negative one entry, with its trips drawn beginning from the uppermost right vertex. (Middle) The tetrahedral-octahedral honeycomb pocket associated to the set of all 3×3 alternating sign matrices. The 4 octahedra are in yellow and correspond to square moves at the four possible square faces of the relevant webs. They are surrounded by 10 blue tetrahedra in one orientation, corresponding to IH moves at white vertices, and 1 red tetrahedron in another orientation, corresponding to the IH move at the black vertex in the left figure. The boundary faces correspond to the vertices on the cycle of green outer edges. (Right) A tableau.

Example 1.6. At another extreme, in [7, §8], it was also shown that certain move-classes are in bijection with plane partitions in the $a \times b \times c$ box. See Figure 2 (middle) for a sample plane partition pocket.

Example 1.7. An example of a different flavor is in Figure 2 (right), which is a pocket associated to the "chained hexagon," which corresponds to the tableau

1	2	3	4	8	12
5	6	7	11	15	16
9	10	14	18	19	20
13	17	21	22	23	24

Using the symmetrized six-vertex conventions in [7], the web move-class is constructed from 12 squares arranged around a central hexagon with all boundary edges pointed inward. The contracted webs in this equivalence class correspond to six 2×2 alternating sign matrices chained together as in [9].

One of the conceptually cleanest properties of pockets is that they are in canonical bijection with 4-row rectangular standard tableaux, without needing to make choices or take equivalence classes. Hence we may write $P(T) = P(\mathcal{C}(T))$ for $T \in \mathrm{SYT}(4 \times c)$. Strictly speaking, pockets are pointed in the sense that the dual vertex of the base face is marked. One may *rotate* a pocket P simply by moving the marked base face to the clockwise next boundary face; pockets remember the orientation of the boundary faces, so this is well-defined. One can *reflect* a pocket by formally reversing this orientation.

Theorem 1.8. *The map $T \mapsto P(T)$ from a 4-row tableau to its pocket is injective. It intertwines tableau promotion with pocket rotation, and tableau* evacuation *with pocket reflection.*

Example 1.9. If the marked vertex in Figure 3 is one of the four corners, the corresponding tableau $T \in \mathrm{SYT}(4 \times 3)$ is indicated in Figure 3 (right). From the symmetry of the pocket, T has order 4 under promotion and is self-evacuating. The other possible marked vertices along the cycle of green outer edges correspond to the promotion powers of L.

Remark 1.10. Promotion and evacuation on $\mathrm{SYT}(r \times c)$ are well-known to generate a dihedral action, though this is mysterious on the level of tableaux. The orbit structure of $\mathrm{SYT}(r \times c)$ under promotion and evacuation is a celebrated result of Rhoades [16]. For $r = 1, 2, 3$, the corresponding webs provide a canonical, graphical model which explains this dihedral action. For $r = 4$, the square move equivalence class of *top* hourglass plabic graphs provides such a model (see [7, Thm. 6.1]). By Theorem 1.8, pockets also provide such a model for $r = 4$, as a geometric realization of the full move equivalence class.

See Theorems 2.1, 2.2, 2.4, 2.8 and 3.3 below for further properties of pockets.

This is an extended abstract only. The full version is in preparation.

2 Combinatorial and topological properties of pockets

Pockets have an extraordinary amount of structure. To make things manageable for the reader, we will incrementally describe this structure in increasing levels of complexity.

2.1 Topology of pockets and distributive lattices

We begin with their basic properties as simplicial complexes.

Theorem 2.1. *Let $\mathcal{C}$ be a move-class of fully reduced 4-row hourglass plabic graphs.*

1. *The pocket $P(\mathcal{C})$ is a flag simplicial complex.*

2. *There are no 4-simplices or higher. All 3-simplices are tetrahedra between embedded dual diskoids of an IH, square, or benzene move.*

3. *$P(\mathcal{C})$ is contractible, hence simply connected.*

Recall pockets come with vertical edges involved in square and benzene moves. Restricting the 1-skeleton of a pocket $P = P(\mathcal{C})$ to its vertical edges gives a disjoint union of paths. We call these paths the *fibers* of P. Every boundary vertex is in a fiber by itself, since square and benzene moves are not applied at boundary faces. Dual diskoids of $G \in \mathcal{C}$ have exactly one vertex from each fiber of P. One may independently fix orientations of each fiber of P, together with certain choices for IH moves, and form a poset on $\mathcal{C}$ where covering relations are given by applying a move in a direction compatible with the given choices. This results in many possible posets on $\mathcal{C}$.

Theorem 2.2. *The following are equivalent.*

1. *$P(\mathcal{C})$ is embeddable in $\mathbb{R}^3$.*
2. *There is some set of choices such that the poset on $\mathcal{C}$ is a distributive lattice.*

Example 2.3. The pockets in Figure 2 may all be embedded in $\mathbb{R}^3$. In the middle case, we recover the distributive lattice of plane partitions exactly. Not all pockets may be embedded in $\mathbb{R}^3$. For example, a variation on the chained hexagon in Example 1.7 is the *chained pentagon*, which instead uses 10 squares arranged around a central pentagon. It has an embedded Klein bottle and so is not embeddable in $\mathbb{R}^3$. See Figure 4.

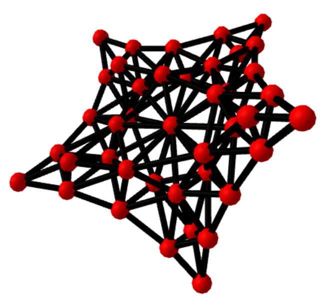

Figure 4: The pocket of a "chained pentagon," which is not embeddable in $\mathbb{R}^3$.

2.2 Piecewise-Euclidean structure of pockets

In addition to the bare simplicial complex structure, pockets possess a piecewise-Euclidean structure as follows. Every triangle in a dual diskoid $D(W)$, or indeed a pocket $P(\mathcal{C})$, has two simple edges and one double edge. In Figure 1, simple edges are in green and double edges are in red. Moreover, every tetrahedron has two disjoint double edges and a cycle of four single edges, all in the same relative positions. Such a tetrahedron can be identified with the fundamental alcove of type $\tilde{A}_4$, say the convex hull of

$$v_1 = (0,0,0,0), v_2 = \frac{1}{4}(3,-1,-1,-1), v_3 = \frac{1}{4}(1,1,1,-3), v_4 = \frac{1}{4}(2,2,-2,-2).$$

This tetrahedron has two long edges of length 1, namely v_1v_4 and v_2v_3, and four short edges of length $\sqrt{3}/2$, namely $v_1v_2, v_1v_3, v_2v_4, v_3v_4$. We may naturally model the triangles in $D(W)$ and the tetrahedra in $P(\mathcal{C})$ on this fundamental alcove, where single edges correspond to short edges and double edges correspond to long edges. This yields a natural piecewise-Euclidean metric on $P(\mathcal{C})$. See, e.g., [1, §1.1] for details.

Recall that a *geodesic* from a to b in a metric space (X, d) is a continuous bijection $\gamma\colon [0, D] \to X$ where $\gamma(0) = a, \gamma(D) = b$, and $d(\gamma(s), \gamma(t)) = |s - t|$ for all $s, t \in [0, D]$. Further recall that a CAT(0) space is a metric space possessing geodesics between arbitrary points such that a geodesic triangle in X satisfies a certain inequality which is intuitively thought of as enforcing non-positive curvature. For simply connected, finite, piecewise-Euclidean complexes, an equivalent condition is that X possesses unique geodesics between arbitrary points [1].

Theorem 2.4. *The pocket $P(\mathcal{C})$ is* CAT(0).

Remark 2.5. Fontaine–Kamnitzer–Kuperberg [6] observed that the dual diskoid of a non-elliptic basis web is CAT(0). Colin Hagemeyer's thesis defined pockets associated to A_1^n and showed they are CAT(0) cube complexes [8, Thm. 1.9].

2.3 Weight-valued distances in pockets

The piecewise-Euclidean structure on $P(\mathcal{C})$ can be enriched using a notion of combinatorial weight-valued metrics explored by Kapovich–Leeb–Millson [10]. More concretely, we will describe an assignment of a partition to each ordered pair of vertices of $P(\mathcal{C})$. These partitions encode the tableau T corresponding to $\mathcal{C}$ under the fundamental bijection [7, Thm. B], along with all powers of promotion, among other information.

First recall the SL(4) weight lattice, $\Lambda := \mathbb{Z}^4/\{(c, c, c, c) \mid c \in \mathbb{Z}\}$. The *dominant weights* are $\lambda \in \Lambda$ with $\lambda_1 \geq \lambda_2 \geq \lambda_3 \geq \lambda_4$. Write Λ_+ for the subset of dominant SL(4)-weights. The *dual* of a weight λ is $\lambda^* := (-\lambda_4, -\lambda_3, -\lambda_2, -\lambda_1) \in \Lambda$, which preserves dominance. The *fundamental weights* ω_i and the dual fundamental weights ω_i^* are

$$\begin{aligned}
\omega_1 &= (1, 0, 0, 0) \equiv (0, -1, -1, -1) = \omega_3^* \\
\omega_2 &= (1, 1, 0, 0) \equiv (0, 0, -1, -1) = \omega_2^* \\
\omega_3 &= (1, 1, 1, 0) \equiv (0, 0, 0, -1) = \omega_1^*.
\end{aligned}$$

We also have $\omega_4 = (1, 1, 1, 1) \equiv (0, 0, 0, 0)$, reflecting the fact that $\wedge^4\mathbb{C}^4 \cong \mathbb{C}$ as SL(4)-modules.

The following non-standard notion of distance will be sufficient for our purposes.

Definition 2.6. Let X be a set and $A \subset X \times X$ where $(a, b) \in A$ if and only if $(b, a) \in A$. A *KLM distance* on A is a function $d\colon A \to \Lambda$ such that for all $(a, b) \in A$,

1. $d(a,b) \in \Lambda_+$ is a dominant weight,
2. $d(a,b) = 0$ if and only if $a = b$, and
3. $d(b,a) = d(a,b)^*$.

To define geodesics for KLM distances, we use the usual partial order on Λ_+. Explicitly, if $\lambda, \mu \in \Lambda_+$ do not have the same sum modulo 4, they are incomparable. Otherwise, normalizing them to have the same sum exactly, the comparison $\lambda \geq \mu$ is done using *dominance order*, i.e., checking if $\sum_{i=1}^k \lambda_i \geq \sum_{i=1}^k \mu_i$ for all k.

Definition 2.7. Suppose A has a KLM distance d. Fixing $(a,b) \in A$, the set

$$\delta(a,b) := \left\{ \sum_{i=1}^{k} d(\gamma_{i-1}, \gamma_i) \mid a = \gamma_0, b = \gamma_k, \text{and } d(\gamma_{i-1}, \gamma_i) \text{ miniscule} \right\} \subset \Lambda_+$$

may have multiple minimal elements, or none. A *KLM geodesic* from a to b is a path achieving a minimal element of $\delta(a,b)$. We say A has *coherent geodesics* if $d(a,b)$ is always the unique minimum of $\delta(a,b)$.

We may begin to build a KLM distance d on a pocket $P(\mathcal{C})$ as follows, extending work of Kuperberg [12] on cut paths for $r = 3$. First, declare that, if F_0, F_1 are adjacent faces of $G \in \mathcal{C}$ with corresponding pocket vertices v_0, v_1, then $d(v_0, v_1) = \omega_m$ if in traveling from F_0 to F_1 we cross an m-hourglass with the white vertex on the right. Observe that $d(v_1, v_0) = \omega_m^* = \omega_{4-m}$. There is a similar rule for vertical edges which we omit.

Theorem 2.8. *Let $T \in \mathrm{SYT}(4 \times n)$. The vertices of the pocket $P(T)$ have a unique KLM distance d extending the above miniscule distances to distances from boundary vertices. This distance possesses coherent geodesics from the boundary. If $v_0 \in P(T)$ is the dual vertex of the base face and $v_1, v_2, \ldots$ correspond to the other boundary faces, then $d(v_0, v_1) \subset d(v_0, v_2) \subset \ldots$ encodes T as a sequence of partitions.*

Remark 2.9. The KLM distance d is computed using a *separation labeling* of P. Separation labelings were introduced for $G \in \mathcal{C}$ in [7] by tracking trips through edges, where the key fact about $d(v_0, v_1) \subset d(v_0, v_2) \subset \cdots$ was proven. We extend them to all vertices of pockets. By uniqueness, the KLM distance is preserved by rotating the pocket. Hence $d(v_i, v_{i+1}) \subset d(v_i, v_{i+2}) \subset \cdots$ encodes the i-th power of promotion of T. Geodesics are sometimes forced to travel through the pocket rather than individual (contracted or uncontracted) webs, which happens already in the 1×1 ASM pocket. Roughly speaking, geodesics may be characterized as avoiding double-crossing any particular trip.

3 Geometric embeddings in affine buildings

A geometric explanation for the KLM distance on pockets involves affine buildings [2]. Buildings were introduced by Tits as combinatorial devices in the study of algebraic groups. Affine buildings are involved in the *geometric Satake correspondence*, which relates the category of equivariant perverse sheaves on the affine Grassmannian of a group such as $\mathrm{SL}(r)$ to its representation category. See [6, §1.2] for a brief overview. We first give a direct, elementary summary of affine buildings, and then state our main pocket embedding result.

3.1 The affine Grassmannian and affine buildings

The *affine Grassmannian* $\mathrm{Gr} = \mathrm{Gr}_r = \mathrm{Gr}(\mathrm{SL}(r)^\vee)$ for the Langlands dual group $\mathrm{SL}(r)^\vee$ is the quotient $\mathrm{Gr} = \mathrm{Gr}(\mathrm{PGL}(r)) = \mathrm{GL}_r(\,\mathbb{C}((t))\,)/t^{-\mathbb{N}}\,\mathrm{GL}(\,\mathbb{C}[[t]]\,)$. Here $\mathbb{C}((t))$ consists of formal Laurent series and $\mathbb{C}[[t]]$ consists of formal power series over $\mathbb{C}$. If $\alpha \in \mathbb{Z}^r/(1^r)$ is a weight, there is a corresponding point $[t^\alpha] \in \mathrm{Gr}$ represented by the matrix $t^\alpha = \mathrm{diag}(t^{\alpha_1}, \ldots, t^{\alpha_r})$. Any group quotient X/Y comes with a natural map to double cosets, $X/Y \times X/Y \to Y\backslash X/Y$ by $(x_1Y, x_2Y) \mapsto Yx_1^{-1}x_2Y$. For the affine Grassmannian $\mathrm{Gr} = \mathrm{Gr}(\mathrm{SL}(r)^\vee)$, the set $\{t^\lambda : \lambda \in \Lambda_+\}$ where λ ranges over the dominant $\mathrm{SL}(r)$-weights forms a complete set of representatives of the double cosets of Gr.

Hence we have a natural KLM distance $d\colon \mathrm{Gr} \times \mathrm{Gr} \to \Lambda_+$ in the sense of Section 2.3. For example, for weights $\alpha, \beta \in \Lambda$, we have $d([t^\alpha], [t^\beta]) = \mathrm{sort}(\beta - \alpha) \in \Lambda_+$. In particular, $d([t^0], [t^\lambda]) = \lambda$. Further note that $d(gp, gq) = d(p, q)$ for all $g \in \mathrm{Gr}$.

The *affine building* $\Delta = \Delta(\mathrm{SL}(r)^\vee)$ is the flag simplicial complex whose vertices are given by $\mathrm{Gr} = \mathrm{Gr}(\mathrm{SL}(r)^\vee)$ and whose edges are given by points $p, q \in \mathrm{Gr}$ such that $d(p, q) = \omega_i$ is a fundamental weight. The subcomplex with vertices $\{[t^\alpha] : \alpha \in \Lambda\}$ forms a *model apartment*, which is a tiling of $\mathbb{Z}^r/(1^r)$ by simplices called *alcoves*. Buildings satisfy various axioms. For instance, any two vertices are contained in some common apartment.

Example 3.1. The affine building $\Delta(\mathrm{SL}(2)^\vee)$ is an infinite tree, where (over $\mathbb{C}$) each vertex is connected to uncountably many adjacent vertices in a fractal pattern referred to as the *Bruhat–Tits tree* (see, e.g., [6, Fig. 1]). For $r > 2$, it is difficult to describe $\Delta(\mathrm{SL}(r)^\vee)$ geometrically.

3.2 Satake fibers, components, and pocket embeddings

Let $\Delta_r = \Delta(\mathrm{SL}(r)^\vee)$. From Section 3.1, a walk on the 1-skeleton of Δ_r by definition means visiting a sequence of points $p_0, p_1, p_2, \ldots \in \mathrm{Gr}$ such that all $d(p_{i-1}, p_i)$ are miniscule. Since we have focused on standard tableaux for the sake of simplicity, we correspondingly suppose $d(p_{i-1}, p_i) = \omega_1$ for all i in such a walk.

The set F_n of loops in the 1-skeleton of Δ from $[t^0]$ to itself with $n := r \cdot c$ such steps each of distance ω_1 can be given the structure of a projective variety and is called a *Satake fiber* [6]. The irreducible components of F are in bijection with rectangular standard tableaux $\mathrm{SYT}(r \times c)$. More precisely, let

$$F_T := \{[(p_0, p_1, \ldots, p_{n-1})] \in F_n \mid p_0 = [t^0], \quad d(p_{i-1}, p_i) = \omega_1, \quad \text{and} \\ d(p_0, p_i) = T_{\leq i} \text{ for } 1 \leq i \leq n\},$$

where $T_{\leq i}$ is the partition consisting of boxes in T with labels $\leq i$ and indices are taken modulo n. Then the irreducible components of F are $\{\overline{F_T} \mid T \in \mathrm{SYT}(r \times c)\}$.

The geometry of F is quite complex. Nonetheless, pockets provide a finite model for each F_T as follows. We first have a natural *geometric rotation* on F_n given by

$$\mathrm{rot}[(p_0, p_1, \ldots, p_{n-1})] := [(p_1^{-1} p_1, p_1^{-1} p_2, \ldots, p_1^{-1} p_{n-1}, p_1^{-1} p_0)].$$

Proposition 3.2 (cf. Thm. 3.5 of [5])**.** *For every $T \in \mathrm{SYT}(4 \times c)$, we have $\mathrm{rot}(\overline{F_T}) = \overline{F_{\mathrm{prom}(T)}}$. Moreover, the following subset is dense in F_T:*

$$U_T := \bigcap_{i=0}^{n} \mathrm{rot}^i F_{\mathrm{prom}^i(T)} = \{[(p_0, p_1, \ldots, p_{n-1})] \in F_n \mid d(p_i, p_{i+j}) = \mathrm{prom}^i(T)_{\leq j}\}.$$

The following key fact shows that pockets generically embed in the affine building.

Theorem 3.3. *For every $T \in \mathrm{SYT}(4 \times c)$, every loop $L \in U_T \subset F_T$ extends uniquely to an embedding $p \colon P(T) \to \Delta_4$ such that $d(p(u), p(v)) = d(u, v)$ for all vertices $u, v \in P(T)$ and the restriction of p to boundary vertices is L.*

Remark 3.4. Since pockets are contractible by Theorem 2.1, they may be thought of as generically providing nice, finite models which "fill in" all possible loops in Δ_4 by Theorem 3.3. In this sense, they encode the geometry of Δ_4.

Acknowledgements

The authors would like to thank Joel Kamnitzer, Greg Kuperberg, Oliver Pechenik, and Stephan Pfannerer for helpful conversations. We are particularly indebted to Greg Kuperberg for the original impetus for this project and the term "pockets."

References

[1] M. R. Bridson. "Geodesics and curvature in metric simplicial complexes". *Group theory from a geometrical viewpoint (Trieste, 1990)*. World Sci. Publ., River Edge, NJ, 1991, pp. 373–463.

[2] F. Bruhat and J. Tits. "Groupes réductifs sur un corps local. II. Schémas en groupes. Existence d'une donnée radicielle valuée". *Inst. Hautes Études Sci. Publ. Math.* 60 (1984), pp. 197–376.

[3] S. Cautis, J. Kamnitzer, and S. Morrison. "Webs and quantum skew Howe duality". *Math. Ann.* **360**.1-2 (2014), pp. 351–390. DOI.

[4] N. Elkies, G. Kuperberg, M. Larsen, and J. Propp. "Alternating-sign matrices and domino tilings. I". *J. Algebraic Combin.* **1**.2 (1992), pp. 111–132. DOI.

[5] B. Fontaine and J. Kamnitzer. "Cyclic sieving, rotation, and geometric representation theory". *Selecta Math. (N.S.)* **20**.2 (2014), pp. 609–625. DOI.

[6] B. Fontaine, J. Kamnitzer, and G. Kuperberg. "Buildings, spiders, and geometric Satake". *Compos. Math.* **149**.11 (2013), pp. 1871–1912. DOI.

[7] C. Gaetz, O. Pechenik, S. Pfannerer, J. Striker, and J. P. Swanson. "Rotation-invariant web bases from hourglass plabic graphs". *Invent. Math.* **243**.2 (2026), pp. 703–804. DOI.

[8] C. S. Hagemeyer. *Spiders and generalized confluence*. Thesis (Ph.D.)–University of California, Davis. ProQuest LLC, Ann Arbor, MI, 2018, p. 106.

[9] D. Heuer, C. Morrow, B. Noteboom, S. Solhjem, J. Striker, and C. Vorland. "Chained permutations and alternating sign matrices—inspired by three-person chess". *Discrete Math.* **340**.12 (2017), pp. 2732–2752. DOI.

[10] M. Kapovich, B. Leeb, and J. J. Millson. "The generalized triangle inequalities in symmetric spaces and buildings with applications to algebra". *Mem. Amer. Math. Soc.* **192**.896 (2008), pp. viii+83. DOI.

[11] A. Knutson, T. Tao, and C. Woodward. "A positive proof of the Littlewood-Richardson rule using the octahedron recurrence". *Electron. J. Combin.* **11**.1 (2004), Research Paper 61, 18. DOI.

[12] G. Kuperberg. "Spiders for rank 2 Lie algebras". *Comm. Math. Phys.* **180**.1 (1996), pp. 109–151. Link.

[13] D. Moskovich. "Who invented diagrammatic algebra?" MathOverflow. Link.

[14] R. Penrose. "Applications of negative dimensional tensors". *Combinatorial Mathematics and its Applications (Proc. Conf., Oxford, 1969)*. Academic Press, 1971, pp. 221–244.

[15] A. Postnikov. "Positive Grassmannian and polyhedral subdivisions". *Proceedings of the International Congress of Mathematicians—Rio de Janeiro 2018. Vol. IV. Invited lectures*. World Sci. Publ., Hackensack, NJ, 2018, pp. 3181–3211.

[16] B. Rhoades. "Cyclic sieving, promotion, and representation theory". *J. Combin. Theory Ser. A* **117**.1 (2010), pp. 38–76. DOI.

[17] J. Striker. "The toggle group, homomesy, and the Razumov-Stroganov correspondence". *Electron. J. Combin.* **22**.2 (2015), Paper 2.57, 17 pages. DOI.